EURASIP Journal on Applied Signal Processing 2005:4, 498–509


# Fingerprint Reference-Point Detection

**Manhua Liu**
*School of Electrical & Electronic Engineering (EEE), Nanyang Technological University, Singapore 639798*
*Email: pg05080538@ntu.edu.sg*

**Xudong Jiang**
*School of Electrical & Electronic Engineering (EEE), Nanyang Technological University, Singapore 639798*
*Email: exdjiang@ntu.edu.sg*

**Alex Chichung Kot**
*School of Electrical & Electronic Engineering (EEE), Nanyang Technological University, Singapore 639798*
*Email: eackot@ntu.edu.sg*

*Received 22 May 2004; Revised 20 August 2004; Recommended for Publication by Montse Pardas*

A robust fingerprint recognition algorithm should tolerate the rotation and translation of the fingerprint image. One popular solution is to consistently detect a unique reference point and compute a unique reference orientation for translational and rotational alignment. This paper develops an effective algorithm to locate a reference point and compute the corresponding reference orientation consistently and accurately for all types of fingerprints. To compute the reliable orientation field, an improved orientation smoothing method is proposed based on adaptive neighborhood. It shows better performance in filtering noise while maintaining the orientation localization than the conventional averaging method. The reference-point localization is based on multiscale analysis of the orientation consistency to search the local minimum. The unique reference orientation is computed based on the analysis of the orientation differences between the radial directions from the reference point, which are the directions of the radii emitted from the reference point with equivalent angle interval, and the local ridge orientations along these radii. Experimental results demonstrate that our proposed algorithm can consistently locate a unique reference point and compute the reference orientation with high accuracy for all types of fingerprints.

**Keywords and phrases:** fingerprint recognition, fingerprint alignment, reference point, orientation smoothing, orientation consistency, reference orientation.

## 1. INTRODUCTION

Fingerprint iscomposed of parallel ridgesand furrows on the tip of the finger. It is widely used for personal identification because of its easier accessibility, uniqueness, reliability, and low cost. Generally, there are two kinds of features for fingerprint recognition: global features such as the special ridge flow pattern and local features like minutia. Consistent extraction of these features is crucial for fingerprint recognition. However, pose transformation, that is, translation and rotation, usually exists in different fingerprint samples of the same finger. One popular solution is to consistently locate a unique reference point and compute a unique reference orientation for translational and rotational alignment of different samples. The singular points, that is, core and delta points (see Figure 1a), are unique landmarks of fingerprint, where the ridge curvature is higher than other areas and the orientation changes rapidly. They are usually used as reference points for fingerprint classification [1, 2]. However, some fingerprints, especially the fingerprints captured with solid-state sensor, contain only partial images with a part of singular points (usually the delta points) left outside the print. In addition, the number of core and delta points differs in different types of fingerprints [1]. For example, the plain arch fingerprint has no singular points while the whorl fingerprint has two core points. To locate a unique reference point consistently for all types of fingerprints and partial fingerprints, we define the reference point as the point with maximum curvature on the convex ridge, which is usually located in the central area of fingerprint (see Figure 1b). Therefore, if core points exist in a fingerprint, the core point on the convex ridge is the reference point. As for the reference orientation, it should be unique for all types of fingerprints and can be consistently determined to reflect the rotation of fingerprint image.

There are many approaches proposed for singular point detection in the literatures and most of them operate on the fingerprint orientation field. The Poincare index (PI) method

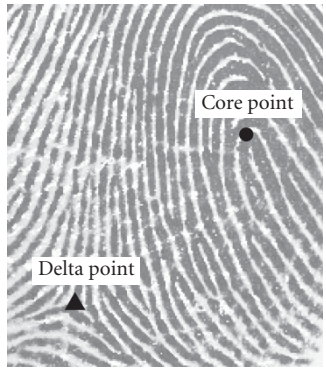


(a)

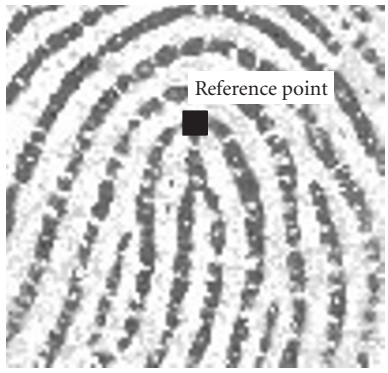


(b)

Figure 1: (a) Core point and delta point. (b) Reference point with maximum curvature on the convex ridge.

[1, 2] is one of the commonly used methods. In this method, the PI of each block is computed by summing up the direction changes around a closed digital curve of the block. This method is efficient, but it is sensitive to noise as the orientation deviation caused by noise will affect the computation of PI, especially when the direction change is near $\pi/2$ or $-\pi/2$. In addition, this method cannot locate the corresponding reference point in plain arch fingerprint because the point with maximum curvature is not core point in a strict sense. Koo and Kot [3] proposed a method of singular point detection based on searching the point with maximum curvature. This method does not work well in poor-quality fingerprint because the computed curvature is sensitive to noise. Jain et al. [4] proposed a sine-map-based method which is to locate a reference point based on multi-resolution analysis of the differences of sine component integration between two defined regions of the orientation field. This method is robust to noise, but the two defined regions are sensitive to the fingerprint rotation. In addition, this method is not effective for reference-point localization in plain arch fingerprint. Park et al. [5] proposed an efficient algorithm of reference-point detection based on orientation pattern labeling. This method is also not consistent to fingerprint rotation and its performance for plain arch fingerprint is inferior to that of the method proposed by Jain et al. [4].

This paper proposes an effective approach to locate a unique reference point consistently and accurately for all types of fingerprints. The reference-point localization is based on multiscale analysis of the orientation consistency which indicates how well the orientations in a neighborhood are consistent with the computed dominant direction. In addition, we propose an improved method for orientation smoothing with adaptive neighborhood, which has better performance in attenuating noise while maintaining the orientation localization than the traditional averaging method. Since the noise-robust orientation field is continuous and has small change except for the high-curvature areas, the reference point defined as the point with maximum curvature of the convex ridge should have local minimum orientation consistency. The curvature direction is employed to differentiate the reference point from other singular points (delta point and the core point in the concave ridge). Furthermore, this paper proposes a method to compute the reference orientation based on analysis of the orientation differences between the radial directions from the reference point and the local ridge orientations along the corresponding radii.

In the following sections, we present in detail our proposed algorithm of reference-point detection and reference-orientation computation. An improved orientation smoothing method is presented in Section 2. Sections 3 and 4 present our proposed approaches of reference-point detection and reference-orientation computation, respectively. The experimental results on the FVC2000 fingerprint database DB2, set A, are presented in Section 5. Finally, conclusions are given in Section 6.

## 2. ORIENTATION FIELD COMPUTATION

Since the reliable orientation field plays a very important role in our proposed algorithm of reference-point localization and reference-orientation computation, it is necessary to address the problem of noise attenuation in the fingerprint orientation estimation.

### 2.1. Orientation estimation

Many methods are proposed for fingerprint orientation estimation in the literatures such as the gradient-based method [6, 7, 8, 9] and the pixel-alignment-based method [1, 10]. The pixel-alignment-based method is to estimate the local ridge orientation of each pixel based on pixel alignments with respect to a fixed number of reference orientations. The total fluctuation of grey values is expected to be the smallest along the local ridge orientation and the largest along its orthogonal orientation. The orientation averaging is employed to estimate the orientation of each image block. The accuracy of the estimated orientation in the pixel-alignment-based method is limited because of the fixed number of reference orientations. The least mean square method of orientation estimation based on the gradients is most widely used to compute the dominant orientation of an image block because of its high efficiency and resolution [6, 7, 8]. Since the gradient phase angle is the orientation with maximum grey value change, it is orthogonal to the local ridge orientation

of each pixel. The orientation of an image block is estimated by averaging the squared gradients to avoid the orientation ambiguity. It was proven that this method is mathematically equivalent to the principal component analysis of the autocovariance matrix of gradient vectors [9]. Therefore, the least mean square method [7] is employed in this work to estimate the orientation of each block. The processing steps are summarized as follows.

(1) Divide the fingerprint image into nonoverlapping blocks of size $w \times w$ pixels ($w = 5$ in our experiment).
(2) Compute the gradients $G_x(u,v)$ and $G_y(u,v)$ of each pixel corresponding to the horizontal and vertical directions. The gradient operator varies from the simple Sobel operator to the complex Marr-Hildreth operator. The Sobel operator is employed in this work for simplicity.
(3) Estimate the orientation of each block $(i,j)$ by averaging the squared gradients as follows:

$$A = \sum_{(u,v)\in W} G_x^2(u,v), \qquad B = \sum_{(u,v)\in W} G_y^2(u,v),$$
$$C = \sum_{(u,v)\in W} G_x(u,v)G_y(u,v), \tag{1}$$

$$\theta(i,j) = \frac{1}{2}\arctan\frac{2C}{(A-B)}, \tag{2}$$

where $W$ is the block of size $w \times w$ pixels.

### 2.2. Orientation smoothing

After orientation estimation, the original grey level image of size $M \times N$ pixels is transformed into the orientation field of size $\text{int}(M/w) \times \text{int}(N/w)$ blocks. The orientation field may still contain some unreliable elements resulting from heavy noise such as scars, ridge breaks, and low grey value contrast. Orientation smoothing is expected to further attenuate noise of the orientation field and compute a reliable orientation field. A statistical smoothing method [11] was proposed that works well to attenuate impulsivelike noise. However, the resolution of the estimated orientation is limited because of the quantified orientation value. The orientation smoothing method based on averaging the unit vectors of doubled orientation over a neighborhood is widely used in orientation smoothing because of its high efficiency and resolution [7]. Obviously, determination of the smoothing neighborhood in this method has great influence on the effectiveness and efficiency of orientation smoothing. If the smoothing neighborhood is too small, heavy noise cannot be well attenuated. Even when the smoothing neighborhood is large, heavy corrupted orientations will still affect the final orientation estimation. In addition, the orientation localization of high-curvature area will be negatively blurred if the smoothing neighborhood is too large. Thus, the orientation is not reliable by using a uniform smoothing neighborhood. This work proposes an improved method for fingerprint orientation smoothing with adaptive neighborhood, which not only maintains the orientation localization of high-curvature area but also has good performance in attenuating noise.

In principle, the determination of the neighborhood in fingerprint orientation smoothing should be based on analysis of the reliability of orientation estimation. A larger smoothing neighborhood is used only if the orientation estimation on small neighborhood is considered to be unreliable. Therefore, an effective measurement is necessary to evaluate the reliability of the orientation estimation. The coherence of the squared gradients was introduced to give a good measure of how well the gradients over a neighborhood are pointing in the same direction [9]. It is computed as follows:

$$\text{Coh} = \frac{\sqrt{(A-B)^2 + 4C^2}}{A+B}, \tag{3}$$

where $A$, $B$, and $C$ are computed in (1). Obviously, the coherence computed by (3) is a good measurement of the reliability of the orientation estimation based on the gradients with the least mean square method. However, in this method, not only the gradient phase angle but also the modulus of the gradient vector will affect the value of the coherence. Although the coherence defined by (3) is normalized by the average grey value contrast $A + B$, the inconsistent grey value contrast in the window $W$ may drastically change the value of Coh. As a result, Coh is sensitive to the inconsistency of grey value contrast and may not correctly reflect the orientation consistency in the window $W$ and the reliability of orientation estimation.

As we are purely concerned with the orientation, orientation smoothing in this work is based on the preliminarily estimated orientation vectors instead of on the gradient vectors. Orientation consistency is introduced that describes how well the orientations over a neighborhood are consistent with the dominant orientation. In a smoothing neighborhood $\Omega(s)$ of each block, orientation consistency is defined as

$$\text{Cons}(s) = \frac{\sqrt{\left(\sum_{(i,j)\in\Omega(s)} \cos\left(2\theta(i,j)\right)\right)^2 + \left(\sum_{(i,j)\in\Omega(s)} \sin\left(2\theta(i,j)\right)\right)^2}}{M}, \tag{4}$$

where $M$ is the number of orientations $\theta(i,j)$ in $\Omega(s)$. If all the orientations in $\Omega(s)$ are exactly directed to one direction, the orientation consistency Cons$(s)$ gives the highest value of 1. If the orientations in $\Omega(s)$ are evenly distributed in $[-\pi/2, \pi/2)$, Cons$(s)$ gets the lowest value of 0. Cons$(s)$ varies between these two extreme situations to provide a quantitative measure of the orientation consistency and reliability. A larger value of Cons$(s)$ reflects more reliable orientation estimation. If each gradient vector in (1) is converted to a unit vector $[G_x(u,v), G_y(u,v)]/\sqrt{G_x^2(u,v) + G_y^2(u,v)}$ to compute $A$, $B$, and $C$, and the gradient phase angle of each pixel is applied as $\theta$ in (4), the coherence in (3) will be equal to the orientation consistency in (4). This equivalence of (3) and (4) does not hold in general. The suggested orientation consistency with the normalized orientation vector of each block is more robust to the inconsistency of contrast than

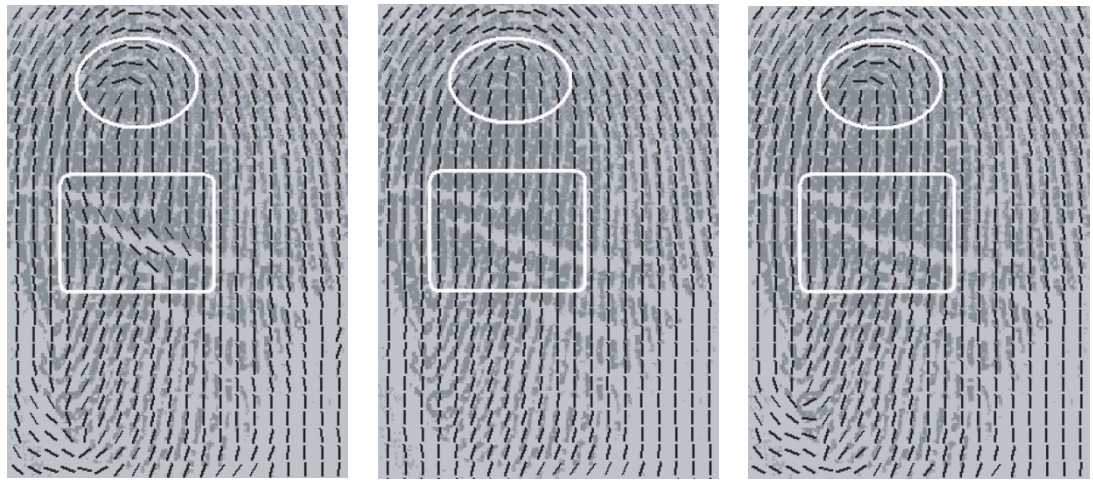

(a) (b) (c)

Figure 2: The orientation fields of a poor-quality fingerprint smoothed in (a) the averaging method on 5×5 neighborhood; (b) the averaging method on $9 \times 9$ neighborhood; and (c) the proposed adaptive smoothing method. The significant orientation errors caused by the $5 \times 5$ and $9 \times 9$ neighborhoods are shown by the white rectangle in (a) and circle in (b), respectively.

the coherence of the squared gradients. Therefore, we use (4) in this work to measure the curvature and the reliability of the orientation estimation for orientation smoothing and reference-point localization.

The basic idea of our proposed orientation smoothing method is to adaptively change the size of smoothing neighborhood based on analysis of the orientation consistency. Fingerprint is composed of parallel ridge flows, and the reliable local ridge orientations change slowly except for some high-curvature areas such as singular region. In practice, we usually get smooth orientation field in most parts of the fingerprint. Sharp orientation changes exist only in either high-curvature or noisy areas. The difference between the high-curvature and noisy area is that the orientation consistency gets larger with increasing the smoothing neighborhood size for the noisy area but is always small with variant neighborhood size for the high-curvature area. Based on this observation, the orientation consistency analysis on varying neighborhood size is used to differentiate the high-curvature area from the noisy area. Only the orientations in the noisy area are further smoothed with the larger neighborhood.

An improved smoothing method with adaptively varied neighborhood is proposed based on analysis of the orientation consistency in this work that works well to attenuate noise while maintaining the orientation localization. Larger smoothing neighborhood is employed to attenuate the heavy noise, while small neighborhood is used in the areas with light noise to maintain the localization. However, the corrupted orientations still affect the final orientation estimation if all the orientations in its neighborhood are included in averaging. The proposed method tries to circumvent the corrupted orientations and use the reliable orientations of its neighborhood to modify the noisy orientations. If the orientation consistency of a block on larger neighborhood is better than that on small neighborhood, the orientations on the outer blocks of the larger neighborhood are more reliable than the orientations on small neighborhood. Therefore, we compute $\mathrm{Cons}(s)$ and the orientation of each block based on the outside surrounding blocks of its $(2s+1) \times (2s+1)$ neighborhood consisting of $8s$ elements to circumvent the corrupted orientations on small neighborhood. The processing steps of the proposed orientation smoothing method for each block are summarized as follows.

(1) Convert the doubled orientation of each block to a unit vector $[\cos(2\theta(i,j)) \sin(2\theta(i,j))]$ and compute $\mathrm{Cons}(1)$ $(s = 1)$ in (4) with $\Omega(1)$ being the outside 8 blocks of its $3 \times 3$ neighborhood.

(2) $s = s+1$. Compute $\mathrm{Cons}(s)$ with $\Omega(s)$ being the outside $8s$ surrounding blocks of its $(2s+1) \times (2s+1)$ neighborhood.

(3) If $\mathrm{Cons}(s)$ is smaller than a threshold (0.5 in our experiment) or smaller than $\mathrm{Cons}(s-1)$, go to step (2) until $s$ reaches its maximum (5 in our experiment).

(4) If $s$ equals its maximum, $\Omega(s)$ is reset to the neighborhood of size $3 \times 3$ blocks.

(5) Compute the smoothed orientation by

$$\theta = \frac{1}{2} \arctan\left(\frac{\sum_{(i,j)\in\Omega(s)} \sin\left(2\theta(i,j)\right)}{\sum_{(i,j)\in\Omega(s)} \cos\left(2\theta(i,j)\right)}\right). \tag{5}$$

In the above processing steps, $\mathrm{Cons}(s)$ is larger than the threshold and $\mathrm{Cons}(s-1)$ indicates that the estimated orientation based on $\Omega(s)$ is reliable. If $\mathrm{Cons}(s)$ of all scales $(s = 1, 2, 3, 4)$ is smaller than the threshold, $\Omega(s)$ is most likely a high-curvature area, we reduce the smoothing neighborhood $\Omega(s)$ to the minimal size $\Omega(1)$. Figure 2 shows the orientation fields with heavy noise smoothed on different

(a) (b)

Figure 3: (a) A whorl fingerprint and its orientation consistency field. (b) A plain arch fingerprint and its orientation consistency field. The white block denotes high orientation consistency.

neighborhoods. From Figure 2a, we can see that heavy noise of the orientation field cannot be well attenuated with small smoothing neighborhood although the orientation localization is maintained. Figure 2b shows that heavy noise is well attenuated with larger smoothing neighborhood, but the orientation localization near the core point is blurred compared with that of Figure 2a. Figure 2c shows that heavy noise is well attenuated while the orientation localization near the core point is maintained by using our proposed adaptive smoothing method. Therefore, our proposed adaptive smoothing method cannot only attenuate well the heavy noise but also maintain the orientation localization of high-curvature area.

## 3. REFERENCE-POINT LOCALIZATION

A good approach of reference-point localization should consistently and accurately detect a unique reference point for all types of fingerprints including plain arch fingerprint in which no singular points exist. In addition, it should be robust to noise such as ridge cracks, scars and so forth. The approach presented below solves these two problems by multiscale analysis of the orientation consistency.

### 3.1. Fingerprint segmentation

Almost all fingerprint images consist of not only the foreground originated from the contact of fingertip with the sensor but also the background, the noisy area on the borders of image, which may produce spurious reference points. Fingerprint segmentation is to decide which part of the image belongs to the foreground and which part belongs to the background. The reference point will be located more accurately if the localization operates only on the foreground of fingerprint image. Thus, fingerprint segmentation plays an important role to reduce spurious reference points. Bazen and Gerez [12] proposed a fingerprint segmentation algorithm based on three pixel features: mean grey value, variance, and coherence. An optimal linear classifier is trained for the segmentation, and morphology is employed as postprocessing to obtain compact clusters and reduce the segmentation errors. This approach works well in fingerprint segmentation. It is applied in this work to segment the foreground from the background of fingerprint image and the three features are computed based on block size ($5 \times 5$ pixels).

### 3.2. Reference-point localization

The reference point in this work is defined as the point with maximum curvature on the convex ridge, which is usually located in the central area of fingerprint. The core point on the convex ridge is the reference point if core points exist in the fingerprint. Although there is no core point in a strict sense in plain arch fingerprint, the point with maximum curvature is always unique and on the convex ridge. As analyzed in orientation smoothing, the orientation consistency is smaller in the high-curvature area than in homogeneous areas (see Figure 3). It can reflect the fingerprint ridge curvature. Therefore, the reference point should have local minimum value of the orientation consistency. However, the orientation consistency in the noisy area is also small that may produce spurious reference points. As previously analyzed in orientation smoothing, to differentiate the high-curvature area from the noisy area, the values of orientation consistency computed on varying neighborhood sizes are analyzed. The orientation consistency values of high-curvature area on varying neighborhood sizes are always small while the orientation consistency of noisy area on the large neighborhood gets larger than that on the small neighborhood. A multiscale analysis (see Figure 4) of orientation consistency is proposed to search the local minimum orientation consistency from large scale to fine scale. To circumvent the corrupted orientations, the orientation consistency of each block on all scales is computed based on the outside surrounding blocks of its neighborhood.

In the multiscale analysis of the orientation consistency, we search the block of local minimum consistency from the largest scale to the finest scale so that noisy areas that produce

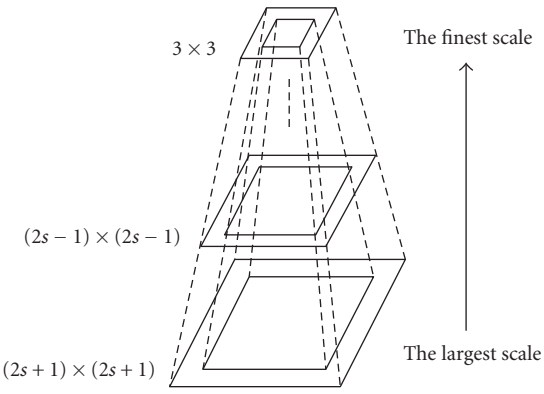


Figure 4: The multiscale analysis of the orientation consistency.

spurious reference points are eliminated. As a fingerprint may contain more than one core point and delta points (see Figure 3a) which also have minimum consistency, we determine the unique reference point according to the direction of curvature.

In the $(2s+1)\times(2s+1)$ neighborhood of block $(i, j)$, we compute

$$dx(s) = \sum_{j=-s}^{s} \cos\left(2\theta(i-s, j)\right) - \sum_{j=-s}^{s} \cos\left(2\theta(i+s, j)\right), \quad (6)$$

$$dy(s) = \sum_{i=-s}^{s} \sin\left(2\theta(i, j-s)\right) - \sum_{i=-s}^{s} \sin\left(2\theta(i, j+s)\right). \quad (7)$$

If both $dx(s)$ and $dy(s)$ of the block with local minimum consistency are larger than 0, this block is the core point on the convex ridge and located as a candidate reference point in the next finer scale. Otherwise, it is not a concern. As a result, the block on the convex ridge with minimum orientation consistency from both large scale and fine scale is located as the unique reference point. The processing steps of the reference-point localization by multiscale analysis of the orientation consistency are summarized as follows (the scale $s$ is initialized as 4 in our experiments).

(1) Compute the orientation consistency $\mathrm{Cons}(s)$ of each block based on the outside $8s$ surrounding blocks of its $(2s+1)\times(2s+1)$ neighborhood.
(2) Find the minimum orientation consistency denoted as $\mathrm{Cons}_{\min}(s)$. If $\mathrm{Cons}_{\min}(s) <= 0.5$, let $T = \mathrm{Cons}_{\min}(s) + 0.15$. Otherwise, $T = \mathrm{Cons}_{\min}(s) + 0.05$.
(3) Select the blocks if their $\mathrm{Cons}(s) < T$.
(4) Compute $dx(s)$ in (6) and $dy(s)$ in (7), respectively, and select the blocks with both $dx(s)$ and $dy(s)$ larger than 0 as the candidate blocks in the next finer scale.
(5) If no candidate blocks for the reference point are located, let $T = T + 0.01$, go to step (3).
(6) Repeat steps (1), (2), (3), (4), and (5) in the selected candidate blocks with $s = s - 1$ until $s = 1$.
(7) Locate the block with minimum orientation consistency $\mathrm{Cons}(1)$ from the selected finest scale blocks as the unique reference point.

In the above processing steps, if $\mathrm{Cons}_{\min}(s) <= 0.5$, the fingerprint most likely contain singular points whose orientation consistency is much smaller than those in other areas. Thus, the threshold $T$ is set to $\mathrm{Cons}_{\min}(s) + 0.15$ to locate the possible reference points. Otherwise, the difference of the orientation consistencies between the reference point and other areas could be small, like the case of plain arch fingerprint. Therefore, the threshold $T$ in this case is set to $\mathrm{Cons}_{\min}(s) + 0.05$, closer to $\mathrm{Cons}_{\min}(s)$.

## 4. REFERENCE-ORIENTATION COMPUTATION

There are few papers concerned with the computation of reference orientation. Bazen and Gerez [9] proposed a method to compute an orientation associated with each detected singular point. In this method, the orientation field near the detected singular point is compared with a standard orientation field model of the same type of singular point. This method performs well if the neighborhood of the detected singular point is very similar to the standard reference model. However, the neighborhood of the detected singular point may have patterns different from the standard model. In addition, this method cannot compute an orientation for the plain arch fingerprints because this type of fingerprint does not belong to any one of the two proposed reference models.

A good reference orientation should be unique and consistently computed for all types of fingerprints to reflect the fingerprint rotation. This work defines 16 radial directions from the reference point with $\pi/8$ interval (see Figure 5a). After analysis of the orientation field in the neighborhood of reference point, the local ridge orientation, which is most parallel to the corresponding radial direction, is unique for the fingerprint whose reference point is core point and can reflect the fingerprint rotation (see Figure 5b). Thus, this local ridge orientation is defined as the unique reference orientation of the core point. For the plain arch fingerprint whose reference point is not core point in a strict sense, there exist two different such local ridge orientations, the average of which is defined as the unique reference orientation (see Figure 5c).

In order to consistently and reliably compute a unique reference orientation, we propose a computing method based on analysis of the orientation differences between the radial directions from the reference point and the local ridge orientations along the corresponding radial. The absolute sine component of the orientation difference is employed to approximate the orientation difference. The mean of the absolute sine component of the difference between the radial direction and the local ridge orientations along the corresponding radial is computed as

$$\mathrm{Var}(k) = \frac{1}{M} \sum_{(i,j)\in\Omega_k} \left| \sin\left(\theta(i, j) - \theta_k\right) \right|, \quad \theta_k = \frac{k\pi}{8}, \quad k = 0, 1, \ldots, 15, \quad (8)$$

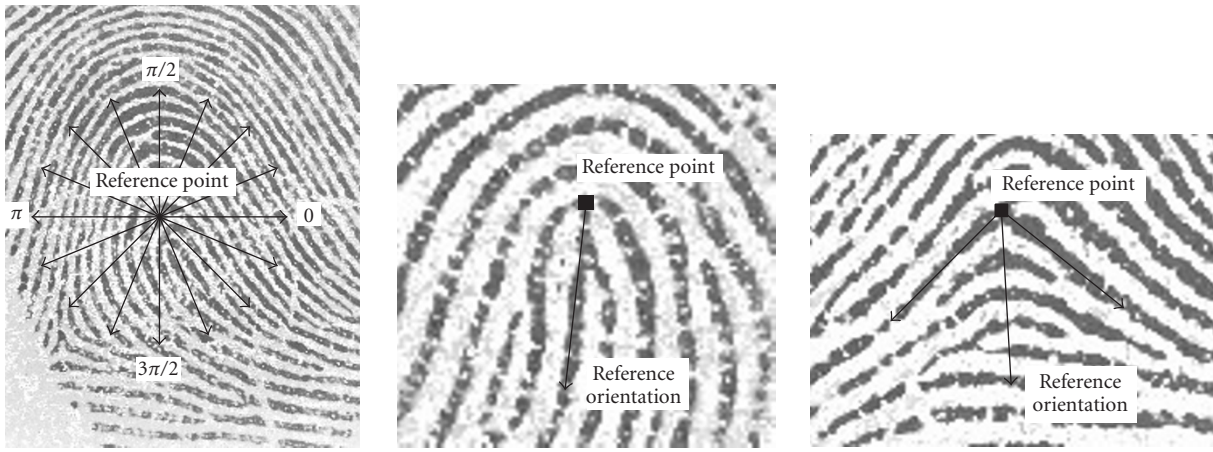


(a) (b) (c)

Figure 5: (a) The 16 radial directions from the reference point. (b) The reference orientation for the core point. (c) The reference orientation for the plain arch fingerprint.

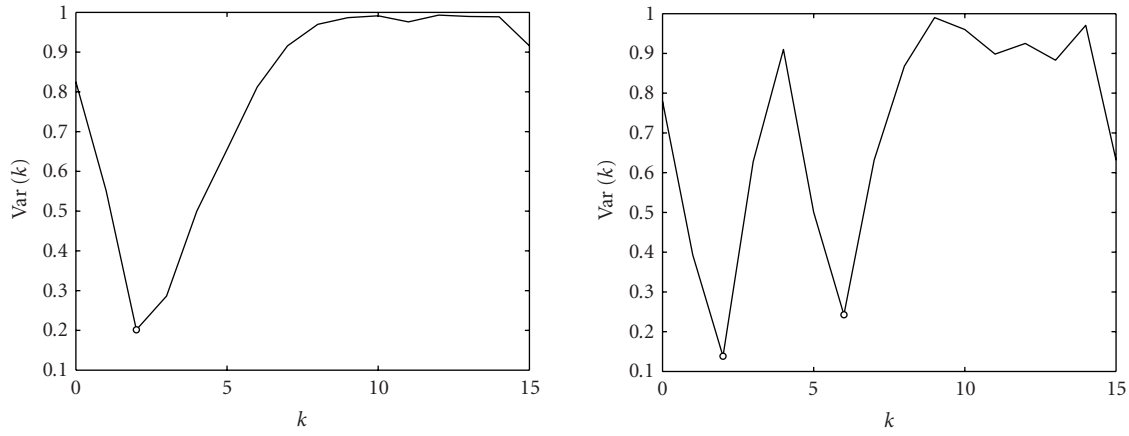


(a) (b)

Figure 6: Var($k$) against $k$ where the circle denotes the minimum: (a) one minimum and (b) two local minimums.

where $\Omega_k$ is a set of $M$ local orientations (denoted by $\theta(i, j)$) along the radial with direction $\theta_k$. It is a rectangle with its length side parallel to the radial and it is symmetric with the radial. Obviously, Var($k$) with range $[0, 1]$ equals 1 when $\theta_k$ is orthogonal to all the orientations in $\Omega_k$ and equals 0 when $\theta_k$ is parallel to them. Therefore, the dominant local ridge orientations of $\Omega_k$ with local minimum Var($k$) are considered to be most parallel to the radial direction $\theta_k$. For the fingerprint whose reference point is core point, only one minimum Var($k$) exists (see Figure 6a). For the plain arch fingerprint, however, two local minimums exist in Var($k$) (see Figure 6b). In order to effectively search the minimum of Var($k$), the size of the orientation set $\Omega_k$ is adaptively changed in this work. The width of $\Omega_k$, the number of blocks along the side orthogonal to the radial, is set to 5 blocks (of size $5 \times 5$ pixels) centered with the radial. The length of $\Omega_k$ is initialized to 4 blocks (the minimum distance between two core points is assumed to be 4 blocks) and adapted by analysis of Var($k$). The processing steps to compute the reference orientation are summarized as follows.

(1) The length and the width of $\Omega_k$ are initialized as 4 and 5 blocks, respectively.

(2) Compute Var($k$) with respect to the 16 radial directions in (8) and find the minimum of Var($k$) as Var($k_{\min}$).

(3) Select the radial directions $\theta_k$ with the Var($k$) $<$ Var($k_{\min}$) + 0.1 as the candidate directions. If two or more such radial directions are continuous with $k$, select the radial direction with minimum Var($k$) among them as one candidate direction.

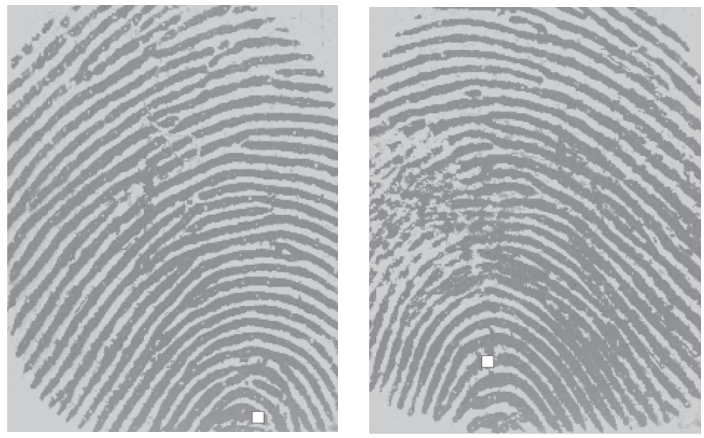

(a) (b)

Figure 7: The identification of partial fingerprint image: (a) the correct identification with the detected point on the boundary of the image; (b) the false identification with the detected point in the internal region of the image.

(4) If more than two candidate directions exist and the length of $\Omega_k$ does not reach the boundary of the image or its maximum (15 in our experiment), add the length of $\Omega_k$ and go to step (2).
(5) Compute the dominant orientation of $\Omega_k$ with respect to the candidate radial directions using the least mean square averaging method. The average of these dominant orientations is the unique reference orientation.

## 5. EXPERIMENTAL RESULTS

The proposed algorithm has been tested on the FVC2000 DB2, set A, in which 800 fingerprint images from 100 fingers (with 8 images from each finger) are captured using a low-cost capacitive sensor. The image size is $364 \times 256$ pixels and the resolution is 500 dots per inch. This fingerprint database contains many poor-quality fingerprints such as the partial images with the reference point left outside and the images with heavy noise like scars, ridge breaks, too wet or dry fingerprints, and so forth. The desired position and orientation of the reference point in each fingerprint are not detected previously by experts. To evaluate the performance of our proposed algorithm quantitatively, we manually locate the desired reference point and the desired reference orientation of each fingerprint.

There are 13 partial fingerprint images in the test database with the reference point left outside. For these images, no reference point should be detected. However, one point with minimum orientation consistency is usually detected in our experiments for each fingerprint. If the detected point is on the boundary of the image (see Figure 7a), this point is unreliable and considered as no reference point being detected. The image is identified as partial fingerprint image. In this way, we correctly identify 11 partial fingerprint images while two partial fingerprints fail being identified as the detected reference points are not located on the image boundary (see, e.g., Figure 7b).

### 5.1. Reference-point localization

In our experiments, the orientation field is computed in the proposed adaptive smoothing method and 4 scales are applied in the multiscale analysis of orientation consistency to locate the reference point. The orientation consistency computation in each scale is based on the outside surrounding $8s$ blocks of $(2s + 1) \times (2s + 1)$ neighborhood and $s$ denotes the corresponding scale of the multiscale analysis.

The reference points detected using different orientation smoothing methods are shown in Figure 8. From Figure 8a, we can see that the averaging method on small neighborhood results in the false reference-point detection due to the heavy noise. Figure 8b shows a significant location error of the detected reference point caused by averaging method on large neighborhood. Our proposed adaptive smoothing method, however, leads to the accurate reference-point detection for both of the fingerprint images.

The position of the reference point is the center pixel of the finally located block. The Euclidean distance between the manually located position and the position located by the algorithm is computed as the distance error of the reference-point localization. Since the reference point determined by human vision may have some deviation from the true reference point, four coarse level measures of the distance error are defined to effectively evaluate the accuracy of reference-point localization in this work. If the distance error of the reference-point localization is not larger than 10 pixels (about 1 interridge), the localization is considered to be accurate as the error may be caused by human vision. If the distance error is larger than 10 pixels but not larger than 20 pixels, it is considered as small error which may be caused by both human vision and algorithm. If the distance error is larger than 20 pixels but not

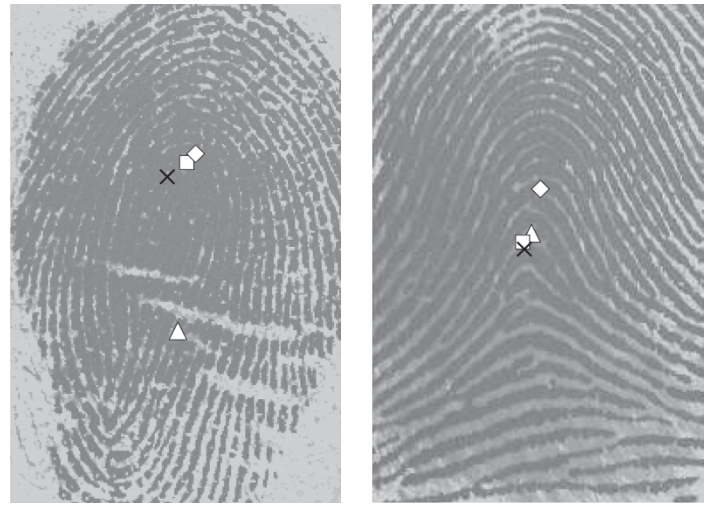

(a) (b)

Figure 8: The reference points detected by different orientation smoothing methods where "×" denotes the manually detected reference point, "△" and "◇" denote the reference point detected by the averaging method on small and large neighborhoods, respectively, and "□" denotes the detected reference point by our proposed adaptive smoothing method.

larger than 40 pixels, it is considered as significant error which may have negative effect on the subsequent processing steps. If the distance error is larger than 40 pixels, most likely a spurious or false reference point is detected that cannot be used for subsequent processing steps. Table 1 shows the accuracy analysis of the reference-point localization for the nonpartial fingerprints of the test database according to the four coarse level measures of the distance error. We can see that the accuracy of the reference point reaches 95.18% if small distance errors can be tolerated in the subsequent processing steps. The experimental results can be further improved by reducing the step size of overlapping blocks. Almost all the significant errors and false detections resulted from the heavy noise of the very poor-quality fingerprints (see Figure 9).

The sine-map-based approach proposed by Jain et al. [4] is a good approach for reference-point localization, and its definition of reference point is the same as that in this work. Therefore, several examples of reference-point localization in our proposed approach are compared with those in the sine-map-based approach (see Figure 10). From Figure 10a, we can see that the detected reference points using the sine-map-based approach are not very consistent among the two fingerprint samples from the same finger due to a slight rotation between them. Figure 10a shows that the detected reference points of these two fingerprint samples by using our proposed approach are more consistent than those using the sine-map-based approach.

Furthermore, the standard deviations of the detected reference points by the two methods are computed to compare their consistencies. Let $Z_r(i)$ and $Z(i)$ be the positions of the manually located reference point and the detected reference point of the sample image $i$ from the same finger, the standard deviation $\sigma$ is computed as

$$\sigma = \sqrt{\frac{1}{M}\sum_{i=1}^{M}\left\| dZ(i) - \frac{1}{M}\sum_{i=1}^{M} dZ(i)\right\|^2}, \qquad dZ(i) = Z(i) - Z_r(i), \tag{9}$$

where $M$ is the number of fingerprint samples (8 in our test database) from the same finger. For the corresponding 8 fingerprint samples from the same finger as shown in Figure 10, the standard deviation $\sigma$ of the reference points detected by the sine-map-based approach is 6.0228, while it is 2.4708 by our proposed approach. The average standard deviation of the whole test database (800 fingerprint images in our test database) by our proposed approach is 11.5109, which is much smaller than that by the sine-map-based approach (19.7800). Therefore, the consistency of the detected reference points by our proposed approach is much better than that by the sine-map-based approach.

Table 1: The accuracy analysis of the reference-point localization for nonpartial fingerprints.

| Distance error (pixels) | The number of fingerprints | The probability |
|---|---|---|
| ≤ 10 | 659 | 0.8374 |
| > 10 and ≤ 20 | 90 | 0.1144 |
| > 20 and ≤ 40 | 25 | 0.0318 |
| > 40 | 13 | 0.0165 |

(a) (b) (c)

Figure 9: Examples of false reference-point detection and the detection with significant error ("×" denotes the manually located reference point and "□" denotes the reference point located by the algorithm).

(a)

(b)

Figure 10: Examples of the reference-point localization by using (a) the sine-map-based approach and (b) our proposed approach ("×," "△," and "□" denote the reference points detected by human experts, the sine-map-based approach, and our proposed approach, respectively).

Table 2: The accuracy analysis of the reference-orientation computation.

| Orientation error | The number of fingerprints | The probability |
|---|---|---|
| $\leq \pi/16$ | 690 | 87.67% |
| $> \pi/16$ and $\leq \pi/8$ | 47 | 5.97% |
| $> \pi/8$ | 50 | 6.35% |

### 5.2. Reference-orientation computation

The difference between the manually detected reference orientation and the reference orientation computed by the proposed approach is computed as the orientation error of the reference-orientation computation. Similarly, three coarse level measures of the orientation error are defined to effectively evaluate the accuracy of the reference-orientation computation (see Table 2). The orientation error larger than $\pi/8$ rads is considered a significant error while the orientation error larger than $\pi/16$ but not larger than $\pi/8$ rads is considered a small error. The orientation error not larger than $\pi/16$ rads is considered an accurate computation. To avoid the ambiguity of the orientation difference computation, the orientation error (OE) is computed as follows:

$$\begin{aligned} \mathrm{OE} &= \min\{|\theta_p - \theta_r|, \pi - |\theta_p - \theta_r|\}, \\ &-\frac{\pi}{2} \leq \theta_p, \quad \theta_r < \frac{\pi}{2}, \end{aligned} \tag{10}$$

where $\theta_p$ and $\theta_r$ are the computed and the manually detected reference orientations, respectively.

From Table 2, we can see that the computation accuracy is 93.65% if the reference orientation can tolerate error up to $\pi/8$. In addition, the accuracy can be further improved if we can improve the accuracy of reference-point localization.

## 6. CONCLUSIONS

This paper develops an effective algorithm to consistently locate a unique reference point and compute a unique reference orientation associated with the reference point for all types of fingerprints. The reference-point localization is based on multiscale analysis of the orientation consistency, while the reference orientation is computed by analysis of the orientation differences between 16 radial directions from the reference point and the local ridge orientations along these radii. In addition, to compute the reliable orientation field, we propose an improved orientation smoothing approach which has better performance in attenuating noise while maintaining the orientation localization of high-curvature area than the conventional averaging method. Finally, experimental results demonstrate that our developed algorithm can consistently locate a unique reference point and compute a unique reference orientation with high accuracy for all types of fingerprints. The located reference point and the computed reference orientation are useful for translational and rotational alignment in fingerprint classification and matching.

## REFERENCES

[1] K. Karu and A. K. Jain, "Fingerprint classification," *Pattern Recognition*, vol. 29, no. 3, pp. 389–404, 1996.

[2] Q. Zhang, K. Huang, and H. Yan, "Fingerprint classification based on extraction and analysis of singularities and pseudoridges," in *Proc. Pan-Sydney Area Workshop on Visual Information Processing (VIP '01)*, vol. 11, pp. 83–87, Sydney, Australia, December 2001.

[3] W. M. Koo and A. Kot, "Curvature-based singular points detection," in *Proc. 3rd International Conference on Audio- and Video-Based Biometric Person Authentication*, vol. 2091 of *Lecture Notes in Computer Science (LNCS)*, pp. 229–234, Halmstad, Sweden, June 2001.

[4] A. K. Jain, S. Prabhakar, L. Hong, and S. Pankanti, "Filterbank-based fingerprint matching," *IEEE Trans. Image Processing*, vol. 9, no. 5, pp. 846–859, 2000.

[5] C.-H. Park, S.-K. Oh, D.-M. Kwak, B.-S. Kim, Y.-C. Song, and K.-H. Park, "A new reference point detection algorithm based on orientation pattern labeling in fingerprint images," in *Proc. 1st Iberian Conference on Pattern Recognition and Image Analysis (IbPRIA '03)*, pp. 697–703, Puerto de Andratx, Mallorca, Spain, June 2003.

[6] M. J. Donahue and S. I. Rokhlin, "On the use of level curves in image analysis," *Image Understanding*, vol. 57, no. 2, pp. 185–203, 1993.

[7] L. Hong, Y. Wan, and A. K. Jain, "Fingerprint image enhancement: algorithm and performance evaluation," *IEEE Trans. on Pattern Analysis and Machine Intelligence*, vol. 20, no. 8, pp. 777–789, 1998.

[8] D. Maio and D. Maltoni, "Direct gray-scale minutiae detection in fingerprints," *IEEE Trans. on Pattern Analysis and Machine Intelligence*, vol. 19, no. 1, pp. 27–40, 1997.

[9] A. M. Bazen and S. H. Gerez, "Systematic methods for the computation of the directional fields and singular points of fingerprints," *IEEE Trans. on Pattern Analysis and Machine Intelligence*, vol. 24, no. 7, pp. 905–919, 2002.

[10] U. Halici and G. Ongun, "Fingerprint classification through self-organizing feature maps modified to treat uncertainties," *Proceedings of the IEEE*, vol. 84, no. 10, pp. 1497–1512, 1996.

[11] B.-G. Kim, H.-J. Kim, and D.-J. Park, "New enhancement algorithm for fingerprint images," in *Proc. 16th International Conference on Pattern Recognition (ICPR '02)*, vol. 3, pp. 879–882, Quebec City, Quebec, Canada, August 2002.

[12] A. M. Bazen and S. H. Gerez, "Segmentation of fingerprint images," in *Proc. Annual Workshop on Circuits, Systems and Signal Processing (ProRISC '01)*, pp. 276–280, Veldhoven, The Netherlands, November 2001.

**Manhua Liu** received the B.Eng. degree in 1997 and the M.Eng. degree in 2002 in automatic control from the North China Institute of Technology and Shanghai Jiao Tong University, China, respectively. Now she is a candidate for the Ph.D. degree at Nanyang Technological University, Singapore. Her research interests include biometrics, pattern recognition, image processing, and so forth.

**Xudong Jiang** received the B.Eng. and M.Eng. degrees from the University of Electronic Science and Technology of China in 1983 and 1986, respectively, and the Ph.D. degree from the University of German Federal Armed Forces, Hamburg, Germany, in 1997, all in electrical and electronic engineering. From 1986 to 1993, he was a Lecturer at the University of Electronic Science and Technology of China where he received two science and technology awards from the Ministry for Electronics Industry of China. He was a recipient of the German Konrad-Adenauer Foundation Young Scientist Scholarship. From 1993 to 1997, he was with the University of German Federal Armed Forces, Hamburg, Germany, as a Scientific Assistant. From 1998 to 2002, he was with the Centre for Signal Processing, Nanyang Technological University, Singapore, as a Research/Senior Fellow, where he developed a fingerprint verification algorithm achieving the top in speed and the second top in accuracy in the International Fingerprint Verification Competition (FVC2000). From 2002 to 2004, he was a Lead Scientist and Head of the Biometrics Laboratory at the Institute for Infocomm Research, Singapore. Currently he is an Assistant Professor at the School of Electrical & Electronic Engineering, Nanyang Technological University, Singapore. His research interests include pattern recognition, image processing, computer vision, and biometrics.

**Alex Chichung Kot** was educated at the University of Rochester, New York, and at the University of Rhode Island, Rhode Island, USA, where he received the Ph.D. degree in electrical engineering in 1989. He was with the AT&T Bell Company, New York, USA. Since 1991, he has been with the Nanyang Technological University (NTU), Singapore, where he is the Head of the Information Engineering Division. His research and teaching interests are in the areas of signal processing for communications, signal processing, watermarking, and information security. Dr. Kot served as the General Cochair for the Second International Conference on Information, Communications and Signal Processing (ICICS) in December 1999 and the Advisor for ICICS '01 and ICONIP '02. He received the NTU Best Teacher of the Year Award in 1996 and has served as the Chairman of the IEEE Signal Processing Chapter in Singapore. He is the General Cochair for the IEEE ICIP 2004 and served as an Associate Editor for the IEEE Transactions on Signal Processing and the IEEE Transactions on Circuits and Systems for Video Technology.